Driving Autonomously Offroad up to 35 km/h

D. Coombs, K. Murphy, A. Lacaze, S. Legowik
Intelligent Systems Division
National Institute of Standards and Technology
Gaithersburg, MD 20899-8230 USA
Tel 301-975-3452 - FAX 301-990-9688
{coombs, kmurphy, lacaze, legowik}@nist.gov

Abstract

A robotic HMMWV (a.k.a. "humvee") drives autonomously offroad at speeds up to 35 km/h (10 m/s, 20 mph). Key features of the implementation that enable driving at these speeds are (1) planning the next 20 m with dynamically feasible trajectories, and (2) increasing the lateral clearance to obstacles at higher speeds. Clothoid trajectories are used in planning the vehicle's immediate path. The speed-indexed clearance requirement improves the safety margin for the vehicle over a range of speeds while retaining the ability to maneuver in close quarters when necessary.

Keywords: Offroad driving, Path planning, Obstacle Avoidance, Vehicle Control

1 Introduction

Two of the challenges facing offroad autonomous driving systems are detecting obstacles in time to respond and driving as fast as the terrain allows. While sensing capabilities are being developed in other efforts, the focus of this work is to drive the vehicle offroad at relatively high speeds.

The NIST HMMWV (Highly Mobile Multipurpose Wheeled Vehicle, Figure 1) drives on benign terrain, where the obstacles are reliably detected by the vehicle's sensors. In the work reported by this paper, the vehicle drives at 35 km/h on rolling grass-covered meadows where the only obstacles were large trees and shrubs. The vehicle is commanded to follow a route given by a sequence of GPS coordinates a few hundred meters apart. As the vehicle drives, it repeatedly plans an obstacle-free path to follow the commanded route in real time using data sensed while the vehicle proceeds.

Figure 1: The NIST HMMWV is actuated and instrumented with a laser range scanner, inertial sensors, and GPS.

The present approach has been in use for over a year at NIST. It has been adopted by the Office of the Secretary of the Defense Demo III UGV (Unmanned Ground Vehicle) program and was demonstrated at the Demo III A (alpha) field trials.

The first main problem the present work addresses is that latencies and cycle rates of sensing and control can lead to instabilities. Clothoid trajectories provide a reliable method for representing the vehicle's path for the next few seconds of driving. The clothoid paths used are dynamically feasible trajectories that account for the initial steering angle and the maximum turn rate of the steering mechanism.

The second main problem is that when high speed driving was attempted with straight-line path segments, the vehicle was brushing past trees at 35 km/h (10 m/s). This issue is addressed by maintaining appropriate lateral clearance to obstacles given planned vehicle speed. Vehicle speed and lateral clearance to obstacles are considered together by the path planner as it plans both steering and speed in the vehicle's trajectory to avoid obstacles.

The impact of this work is that the sensorimotor integration and control requirements for driving offroad at high speeds have been met in anticipation of future advances in terrain sensing and interpretation capabilities.

2 Related Work

Many previous efforts have accomplished high-speed driving on roads [0], [0], [0]. These onroad behavior generators deliberately exploit road characteristics by using explicit models of roads. Current implementations for onroad driving consist primarily of lane detection and following. Onroad obstacle avoidance is in early stages of development. It has so far been limited to interacting with other vehicles traveling in the same direction as the autonomous vehicle. In contrast, offroad driving implementations

Proceedings of the 2000 Intelligent Vehicles Conference, the Ritz-Carlton Hotel, Dearborn, MI, USA, October 4-5, 2000.

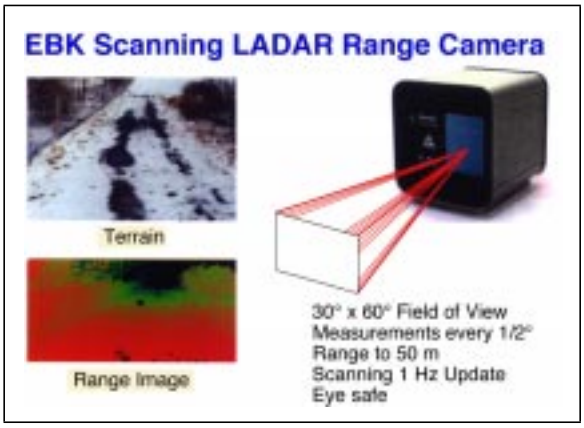

Figure 2: The LADAR range camera scans over its field of view in about 0.5 s, collecting 8192 range measurements that can be treated as a range image or as a collection of 3D points.

consist of detecting and avoiding arbitrary obstacles in an unstructured environment.

Many approaches to onroad driving use several independent specialized behavior generators and then combine their results with some arbitration scheme. In contrast, the present work fuses all information in the world model and generates behavior with a single planner for each planning level of detail. In addition, our planning methodology is not limited to clothoids, and more sophisticated models can be accommodated. This issue becomes crucial for handling challenging situations, such as slippery terrain, in which clothoids would provide poor approximations to the trajectories the vehicle will exhibit. The key fact that enables the use of models more complex than clothoids is that our approach does not rely on merging behaviors represented by a fixed list of clothoidal or circular path segments.

Previous offroad efforts have delivered impressive results [0], [0], [0], but none has focused specifically on driving as fast as possible by selecting relatively benign terrain.

The fastest previous results driving offroad have been delivered by the PRIMUS (PRogram of Intelligent Mobile Unmanned Systems) program, which recently demonstrated offroad autonomous driving up to 25 km/h with a small tracked vehicle, the Wiesel 2 [0]. Path following and obstacle avoidance capabilities similar to the present work were displayed. A scanning LADAR (LAser Detection and Ranging) range imager similar to the one used on the NIST HMMWV, but faster (4 Hz), was used to detect obstacles. Because it is a tracked vehicle, Wiesel 2 has the ability to drive over obstacles that the HMMWV must avoid. Additionally, the sensing rate being 4 times faster gave the PRIMUS vehicle 4 times more opportunities to detect an obstacle in the same amount of time.

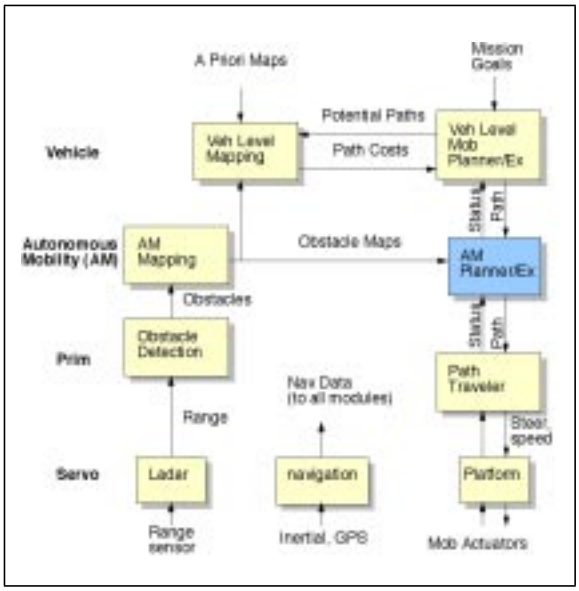

Figure 3: The Mobility software architecture is composed of levels and functional divisions. Time horizon increases at higher levels. SPWM (Sensory Processing and World Modeling) modules, on the left, interpret sensor data in the context of the vehicle's current situation and update the world model. BG (Behavior Generation) modules make, execute, and monitor plans using the world model. This paper primarily focuses on the highlighted AM Planner/Executor module.

Kelly [0] provides an excellent analysis of the challenges offered by high speed offroad driving and a detailed solution. However, it has never run a real vehicle at high speed in real time.

The present work focuses on performing as much of the necessary analysis as possible offline in order to minimize the computations required online.

3 Approach

The mobility software architecture is sketched in Figure 3. The mobility software is designed in accordance with the NIST RCS (Real-time Control System) Reference Model Architecture. [0] [0] The focus of the present work is the AM (Autonomous Mobility) Planner/Executor. Plans at higher levels are provided from mission plans and Vehicle-level subsystems. Obstacle locations and the vehicle's position and orientation are provided by onboard sensors. These data and plans are integrated in the world model. AM planning takes place in a local vehicle reference frame, and the planned path is followed by the Path Traveler.

The AM Planner is presented a path by the Vehicle Level Mobility Planner based on the best information available to it. This is augmented with the latest Subsystem level obstacle map, based on data integrated from the range camera (Figure 2 and Figure 4) vehicle odometry, GPS (Global Positioning System), and inertial sensors. Obstacle detection and

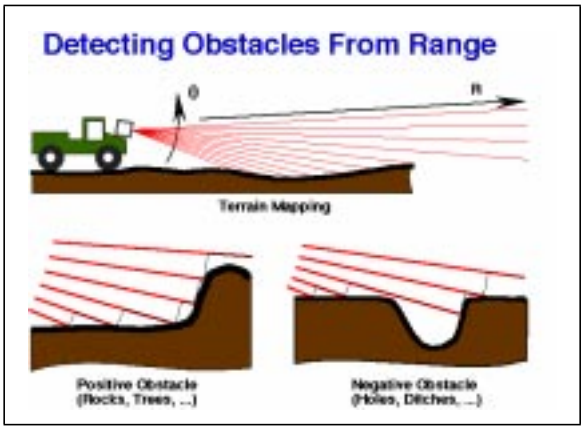

Figure 4: Obstacles are detected in range data by sweeping up each column of pixels in the range data in search of range discontinuity. Positive obstacles present clusters of similar range. Negative obstacles produce range gaps.

terrain analysis are based on data from the time-of-flight scanning LADAR range camera [0]. The range data and vehicle position and attitude are integrated in a North-oriented reference frame (Figure 5).

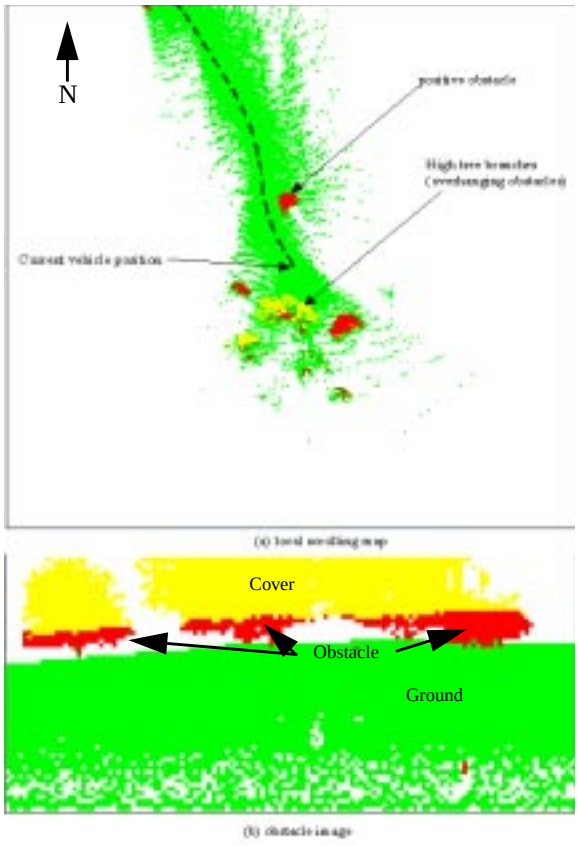

Figure 5: A north-oriented obstacle map (a) integrates data over time. A classified LADAR image (b) shows ground on which the vehicle can drive, obstacles to avoid, and cover under which the vehicle could be concealed from aerial view.

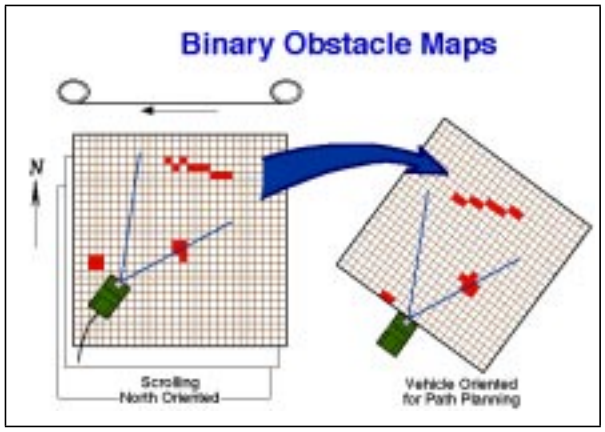

Figure 6: The autonomous mobility level accumulates obstacles (red) and cover in a scrolling north-oriented map. The vehicle's path is planned in a vehicle-oriented map that is located where it is predicted that the vehicle will begin following the path that is being planned.

These data are transformed into a vehicle-oriented local coordinate frame whose origin is located at the position where the vehicle is predicted to be when it begins to follow the path that is being planned (Figure 6) [0]. This local map covers 50x50 m, with each cell 0.4x0.4 m. A large set of paths the vehicle is capable of following are precalculated off-line (Figure 7). Often only < 10% of these edges are searched in each online planning cycle because only those that meet the initial conditions are considered.

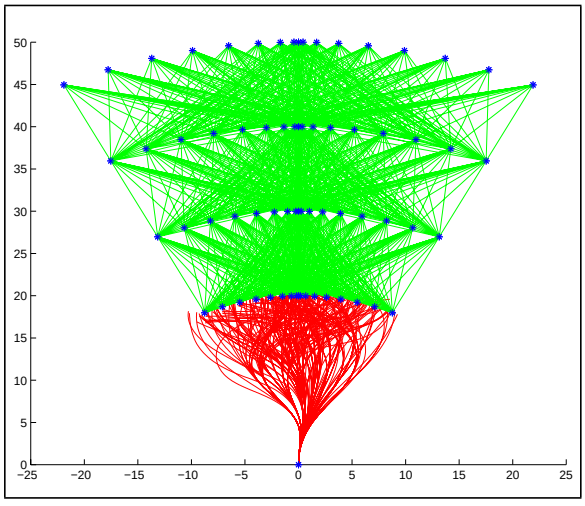

Figure 7: This vehicle-oriented "ego-graph" shows the precomputed paths that are searched during online path planning. The first 20 m are densely-connected with smooth trajectories that are dynamically feasible. For clarity, only those for a single initial steering angle (turned to the right) are shown. The last 30 m are connected by straight lines. The complete set of paths contains $11x17^5$ (over 15 million) trajectories in a graph of approximately 4000 edges, and most of the edges are in the first 20 m.

AM (Autonomous Mobility) path planning selects the lowest-cost obstacle-free path among these. Part of the computations are performed offline, and part are

performed online. Offline, a trajectory-to-cell table is calculated that relates each path segment to the local vehicle-oriented map cells through which it passes. Each path segment has a width to account for the vehicle's width and some clearance. The trajectory-to-cell relation is inverted and is represented by a cell-to-trajectory table. Online, the cell-to-trajectory table is used to discover which path segments are blocked by obstacles (Figure 8). A path segment is clear only if it is completely free of obstacles. Each obstacle's cell location is looked up in the cell-to-trajectory table to determine which path segments are blocked by that obstacle. The online planning runs at 4 Hz.

3.1 Clothoidal paths

Simple straight-line segments worked at low speeds, but were unstable at high speeds. Latencies and discretization contributed to the problem. A key component of the solution is planning the first few seconds of behavior with paths that are dynamically feasible given the response characteristics of the steering mechanism. The dynamic feasibility of the paths enables the vehicle to follow the paths more closely. Therefore the tolerances on path clearance can be tighter.

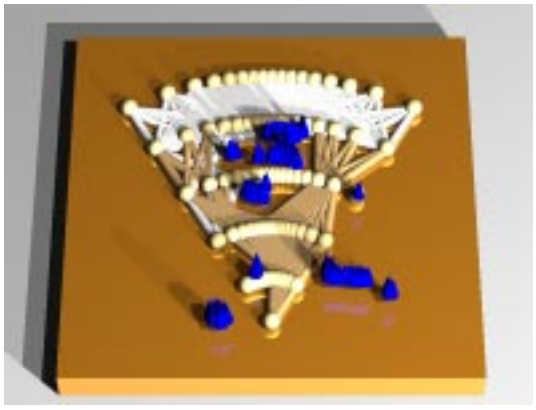

(a) obstacles blocking paths, via cell-to-trajectory table

(b) least costly path found by searching the graph

Figure 8: (a) Local path planning first eliminates path segments that are blocked by the obstacles in the vehicle-centered map. (b) The least costly path is then found by searching the path segments remaining in the graph.

The paths extending 20 m from the vehicle consist of sequences of clothoidal segments. These paths were generated by simulating the vehicle trajectories resulting from a sequence of steering rate commands. They were generated for a range of initial steering angles and a range of vehicle speeds (Figure 9). A *clothoid* is a curve whose curvature varies linearly with arc-length, *i.e.*, a constant curvature plus a constant rate of change of curvature: $\gamma = \frac{1}{r} = c_0 + c_1 s$, where γ is the curvature, r is the radius of curvature, and s is distance traveled. Clothoids correspond to changing the steering angle smoothly at constant speed. Constant curvature with no change $(c_0 = k, c_1 = 0)$ represents a fixed angle of the steering wheels. Nonzero c_1 represents turning the steering wheels at a constant rate. The model includes the limits on steering rate, which is limited by the speed of the steering wheel actuator. The model also includes soft limits on steering angle as a function of vehicle speed. In addition the model includes understeer (in which the vehicle turns less at higher speeds for the same steering angle due to wheel slippage, tire deflection, *etc.*). This model makes the unrealistic assumption that acceleration of the steering actuator is infinite, but it is a fair approximation.

A set of 20 m clothoid sequences is used to cover a range of initial vehicle velocities and turning rates. An example is shown in Figure 9. This figure highlights

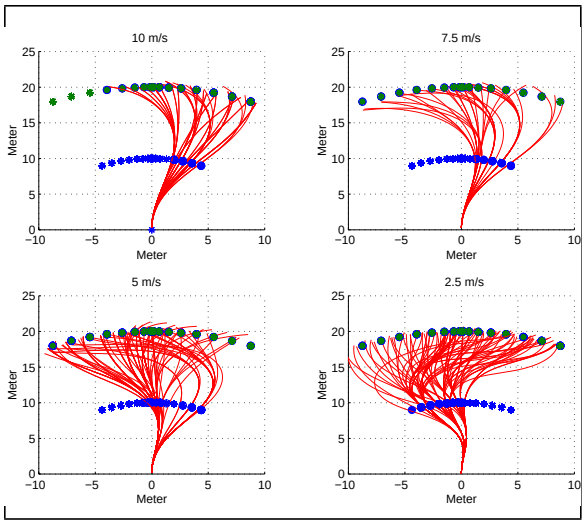

Figure 9: An sample set of path segments: These path segments are a complete set of 20 m paths given an initial steering angle to the right. Additional path sets are computed for several other initial steering angles. The asymmetry is explained by the initial condition. The paths labeled 10 m/s are feasible at speeds up to 10 m/s. The paths labeled 7.5 m/s are the paths that are feasible at speeds up to 7.5 m/s but not greater.

the importance of modeling the limits of steering rate. At 10 m/s, nearly one-third of the terminal points on the 20 m radius and two-thirds of the points on the 10 m radius are unreachable given the initial steering angle and the steering rate limit.

The set of segments feasible for 10 m/s travel is assumed to be traversable at lower speeds as well. A large space of trajectories can be considered in online path selection with this method. Beyond 20 m, segments to 50 m range are treated with straight line approximations because the AM path will be replanned before those segments are traversed.

Recall that only obstacle-free paths are searched online because those blocked have already been eliminated from consideration. Higher speed paths are preferred to lower speed paths because they are smoother and have more clearance. Clearance has already been considered because the faster paths are wider, as described in Section 3.2. Paths slower than the vehicle's current speed will not be considered because the vehicle is traveling too fast to execute the tight turns that are feasible only at lower speeds.

3.2 Speed-indexed clearance

Speed-indexed clearance solves two problems that occurred when straight-line path segments where used in the first attempts to drive at high speed. First, the vehicle drove too close to obstacles at high speeds. The vehicle would brush its mirrors and antenna mounts against tree branches when it was driving fast as well as slow. Not only did this behavior risk damaging equipment on the vehicle, but also it left little room for error.

The second problem was that the path would sometimes become blocked when the vehicle was driving closely around an obstacle near the path. This could occur because new data showed the obstacle to be larger than previously sensed, placing it within the path safety margin. Another source of this problem was that the vehicle-oriented map could move with the vehicle such that the obstacle had expanded into a previously clear cell. This could block all the vehicle's available paths when the vehicle was near the obstacle. When the vehicle was far enough from the obstacle, a sharper curve could be used at lower speed to take the vehicle away from the obstacle. This problem would also be lessened by adding cost to a path as a function of its proximity to obstacles, rather than a binary blockage function.

These problems are addressed in the present work by increasing clearance requirements at higher vehicle speeds. Lateral clearance of each path segment is related to the segment's speed. Each clothoidal path segment's width is increased by 0.8 m of additional clearance (the width of two 0.4 m cells) for each step increase in speed above the minimum 2.5 m/s. Path width ranges from 3 m for 2.5 m/s paths to 5.4 m for 10 m/s paths. The straight-line segments from 20 m to 50 m are all considered to be traversable up to 10 m/s, so they have the same 5.4 m width as the 10 m/s clothoids. The concept is illustrated by Figure 10.

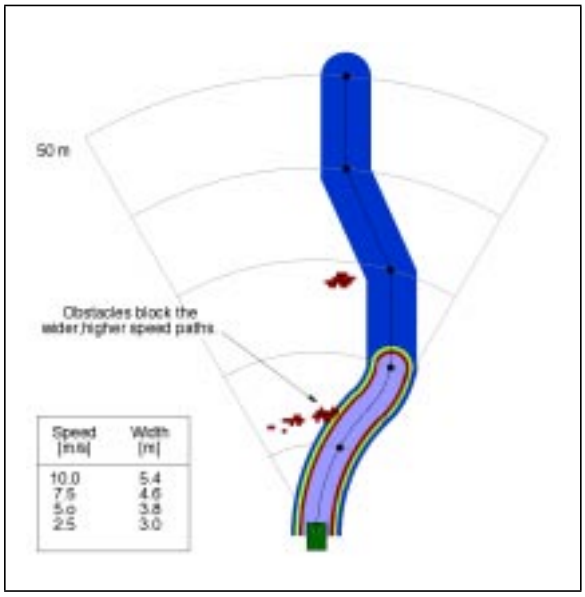

Figure 10: Speed-indexed path clearance concept is illustrated approximately. At slower speeds, the vehicle has liberty to veer more sharply to avoid obstacles. Similarly, the vehicle is able to negotiate a narrower gap. The path width associated with each path segment is related to the speed at which the path would be driven.

This policy is implemented by using speed-indexed path segment widths in building the trajectory-to-cell and cell-to-trajectory tables. The wider paths cover more cells in the trajectory-to-cell table, and when the mapping is inverted, more cells can block the path in the cell-to-trajectory table. An obstacle in any cell through which a trajectory passes will block that path segment. This increases the clearance between the vehicle and obstacles at higher vehicle speeds. Even if higher-speed paths should become blocked as the vehicle approaches an obstacle, there should be enough clearance for lower-speed paths to remain feasible, allowing the vehicle to proceed past the obstacle.

A common approach that has similar results is to grow obstacles rather than the vehicle path width. In these cases, the vehicle may be treated as a point. However, growing obstacles would have been a more expensive online computation for us. By growing the vehicle path width, the computation is performed offline, and the online cost is embedded in the cost of using the cell-to-trajectory table to eliminate paths blocked by obstacles.

4 Conclusion

These techniques enabled the vehicle to travel over rolling meadows at speeds up to 35 km/h (10 m/s) while avoiding obstacles that were well within the

vehicle's current sensing capabilities, such as large trees and shrubs. The vehicle had no *a priori* knowledge of the obstacles.

The vehicle's top speed of 10 m/s is limited by the range, angular resolution, and update rate of the LADAR. Large obstacles are reliably detected at around 40 m, providing at most 4 s of advance information about obstacles. In addition, latencies associated with the LADAR's 1 Hz scan rate, data processing, and 4 Hz path planning further reduce the lookahead to just over 3 s. Doubling the vehicle's speed would cut the lookahead to 1.5 s to 2 s. To increase the lookahead, it would be necessary to detect obstacles at greater ranges and reduce latencies (*e.g.*, by increasing sensor update rates).

In general, it is probably desirable for the vehicle to negotiate the terrain in addition to avoiding obstacles. This emphasizes the notion that terrain is traversable at some speed depending on its particular characteristics, rather than assuming that terrain is smooth but dotted with obstacles. This will require a more sophisticated terrain analysis and planning model than the binary model used presently. However, the more complex model should enable the system to address another challenge looming on the horizon. For many applications, it is necessary to maneuver the vehicle in tight quarters, in some cases even to the point of driving through overhanging branches and pressing through brush. It is hoped that a general solution could address the entire spectrum from high speed driving over varied terrains to maneuvering in tight quarters.

Acknowledgments

Development of an intelligent perception and vehicle navigation control system is a jointly sponsored effort which leverages technology from the NIST Intelligent Machines Initiative program and receives financial support from the Office of the Secretary of the Defense Demo III UGV program and the AUTONAV (Autonomous Navigation) research project agreement between the German Ministry of Defense and the United States Department of Defense. This work has benefited from innumerable discussions with Tsai-Hong, Stephen Balakirsky, Maris Juberts, Jim Albus, John Evans, Marilyn Abrams, Tommy Chang, and other Demo III colleagues.

References

[0] Albus, J.S. "4-D/RCS Reference Model Architecture for Unmanned Ground Vehicles," *Proceedings of the SPIE Vol. 3693 AeroSense Session on Unmanned Ground Vehicle Technology*, Orlando, FL, April 7-8, 1999

[0] Albus, J.S. "A Theory of Intelligent Systems," *Control and Dynamic Systems*, Vol. 45, pp. 197-248, 1991

[0] Chang, T., Hong, T., Legowik, S., Abrams, M.N. "Concealment and Obstacle Detection for Autonomous Driving," *Proceedings of the Robotics & Applications 1999 Conference*, Santa Barbara, CA, October 28-30, 1999

[0] Dickmanns ED. "Computer vision and highway automation," *Vehicle System Dynamics* 31: (5-6), pp. 325-343, June 1999

[0] Hatipo, C., Redmill, K., Ozguner, U., "Steering and Lane Change: A Working System," *IEEE Conference on Intelligent Transportation Systems*, pp. 272-277, November 1997

[0] Kelly, A. *An Intelligent Predictive Control Approach to the High Speed Cross Country Autonomous Navigation Problem*, Ph.D. Thesis, the Robotics Institute, Carnegie Mellon University, Pittsburgh, PA, 1995

[0] Lacaze, A., Moscovitz, Y., DeClaris, N., Murphy, K. "Path Planning for Autonomous Vehicles Driving Over Rough Terrain," *Proceedings of the ISIC/CIRA/ISAS 1998 Conference*, Gaithersburg, MD, September 14-17, 1998

[0] Schwartz, I. "PRIMUS: an autonomous driving robot," *Proceedings of the SPIE Vol. 3693 AeroSense Session on Unmanned Ground Vehicle Technology*, Orlando, FL, April 7-8, 1999

[0] Thorpe, C., Ed. *Vision and Navigation - The Carnegie Mellon Navlab*, Kluwer Academic Publishers, 1990

[0] Turk, M.A., Morgenthaler, D.G., Gremban, K.D., *et al*. "VITS - A Vision System For Autonomous Land Vehicle Navigation." *IEEE Transactions on Pattern Analysis and Machine Intelligence* 10: (3), pp. 342-361, May 1988